Published in final edited form as:
Orthod Craniofac Res. 2009 August ; 12(3): 149–158. doi:10.1111/j.1601-6343.2009.01448.x.

Morphological integration of the skull in craniofacial anomalies

J.T. Richtsmeier and
Department of Anthropology, Pennsylvania State University, University Park, PA, USA, Center for Craniofacial Development and Disorders, Johns Hopkins University School of Medicine, Baltimore, MD, USA, and Center for Functional Anatomy and Evolution, Johns Hopkins University School of Medicine, Baltimore, MD, USA

V.B. DeLeon
Center for Functional Anatomy and Evolution, Johns Hopkins University School of Medicine, Baltimore, MD, USA

Abstract

Objectives—To understand how surgical interventions impact the organization and internal integration of the major components of the skull, we address the functional and developmental relationships during perinatal development.

Methods—A number of methods for quantifying modularity and integration of morphological data are available. Here, measures derived from three-dimensional computed tomographic (CT) images are used to investigate the statistical relationships among measures of the cranial vault, face and cranial base. First, we establish the pattern of associations among quantitative measures in a sample of children unaffected by a craniofacial anomaly. We statistically compare these normative patterns of cranial integration to those of a sample of children with a facial anomaly (complete unilateral complete cleft lip and palate), and to children with a neurocranial anomaly (isolated sagittal synostosis). Finally, we test whether surgery affects the strength and pattern of associations among measures within the cranial base in the affected children.

Results—Our analyses reveal strong internal integration of the cranial base in unaffected children and in our samples of unoperated cleft lip and palate, and sagittal synostosis. Post-operatively, the magnitude of integration of the cranial base is reduced relative to the pre-operative condition in both samples of children with craniofacial anomalies.

Conclusion—Our results show how the cranial base adjusts to its broader structural context, and provides added support for the developmental and structural integration of cranial base with both cranial vault and face.

Keywords

cleft lip and palate; computed tomography; landmark data; morphological integration; sagittal craniosynostosis; three-dimensional

Correspondence to: Joan T. Richtsmeier, Department of Anthropology, The Pennsylvania University, University Park, 16802 PA, USA, jta10@psu.edu.

Clinical relevance

In this study, we establish the pattern of covariation among measures of the cranial base, cranial vault and facial skeleton using data from 3D CT scans in unaffected children and those affected by craniofacial anomalies. The cranial base reveals the strongest patterns of covariation, or integration of morphological traits, in all of our samples. Post-operatively, patterns of covariation change among the components of the skull, demonstrating non-local effects of craniofacial surgery. A better understanding of integration within the skull contributes to the body of knowledge that informs prediction of surgical outcomes.

Introduction

Many craniofacial conditions involve malformations of the bones of the skull, resulting in functional and aesthetic consequences that are managed by surgical intervention. Skull anomalies are often described as independent features (clefts, hypoplasias, suture closures, etc.) with little information on how the dysmorphic trait affects the overall craniofacial complex. In contrast, outcomes are often evaluated within a broader framework that includes the entire craniofacial complex. Understanding the development and interdependence of a structural anomaly, both before and after intervention, can add to the planning of reconstructive therapeutics, thereby enhancing outcome.

Development of the skull involves precisely timed migrations and relations of cell populations, coordinated patterns of differentiation and growth of tissues and biomechanical interactions (1–3). Although the importance of the interaction of soft and hard tissues in development and evolution of the head has long been recognized, the skull has been singled out as a structure worthy of independent analysis. The impact that dysmorphology or deformation of one of the skull regions can have on the others is shown in studies of non-local effects of 1) culturally motivated cranial deformation cradle boarding (4–6); 2) congenital cranial anomalies in humans and animal models (7–10); 3) analyses of the secondary effects of cranial vault surgery (11–13).

‘Morphological integration’ (MI) is the quantitative study of the association between complex traits and provides measures of covariation that infer developmental and/or functional relationships. Analysis of MI attempts to demarcate those subsets of phenotypic traits that strongly co-vary as a window into developmental relationships that underlie these statistical associations. The concept of MI was introduced in the mid 1950s (14) but has earned new attention recently (15,16). Olson and Miller (14) originally predicted and then demonstrated that developmentally and functionally related traits are relatively highly correlated in the phenotype and that the magnitude of the correlation reflects the strength of the biological association.

The concepts of MI and modularity are used to describe the coincident nature of coordination (integration) and relative autonomy (modularity) of parts of an organism (17). Modularity refers to the autonomy of units, or modules within an organism that are integrated on the basis of genetic, developmental, structural or functional relationships. Modules may be hypothesized based on prior biological information or characterized through patterns of trait interaction exhibiting strong intercorrelations (18).

Most biological systems have a modular organization, and the skull is no exception. Traditionally, two principal modules of the skull are defined: the braincase (neurocranium) and the facial skeleton (viscerocranium). Modules are in turn composed of sub-modules so that modularity is hierarchical (e.g. neurocranium is composed of cranial vault and cranial base). The structure of each module is coordinated and integrated, so that change in one aspect of a module (submodule) is answered with a coordinated change in other parts of the module.

The identification and delimitation of modules is dependent upon the context of the research questions being addressed. Consequently, different sets of modules with very different boundary conditions might be defined for the same biological system depending upon whether the research question concerns development, evolution, genetics or functional anatomy of the system. In this study, we adopt the traditional view of modularity in the skull, which is a composite of anatomic and functional information. The facial skeleton houses several special sense organs while the neurocranium envelops the brain. The cranial vault provides protection for the superior aspect of the cerebrum and cerebellum while the cranial base supports the

ventral aspect of the central nervous system, provides passage of neurovascular structures to their targets and serves as a scaffold for attachment of pharyngeal structures.

We use MI to reveal the strength of association between cranial vault, cranial base and face in skulls of infants unaffected by any craniofacial anomaly (our 'unaffected' sample), in infants with complete unilateral cleft lip and palate (UCLP), and in infants with sagittal craniosynostosis (ISS). Importantly, we already have ample evidence pertaining to the morphological differences among these three craniofacial phenotypes, e.g. (13,19,20). In the current analysis, we seek to understand how patterns of relationships within and between the three major parts of the skull are affected by an anomaly and by a surgical correction of that anomaly. Our null hypothesis is that patterns of MI are similar among all samples that we analyse. Statistical evaluation of differences in patterns of MI reveals how the three regions respond to one another during the growth process before and after surgery.

Materials and methods

Samples and data

The study samples include computed tomography (CT) images of the heads of human infants diagnosed with ISS, a sample of infants with UCLP and a control sample of unaffected individuals. Head CT images of unaffected and ISS children were previously acquired for clinical purposes at the Johns Hopkins Hospital, Baltimore, MD; Children's Hospital, St Louis, MO and Oklahoma Children's Hospital, Oklahoma City, OK. Head CT images of infants with UCLP were previously acquired and archived at Chang Gung Memorial Hospital. Data collected from the images were acquired and analysed under IRB protocols approved at the institutions named above and at the Pennsylvania State University. Data pertaining to the ethnicity of the unaffected and ISS study samples were not available, but individuals that make up the UCLP sample are all of Taiwanese Chinese ethnicity.

Unaffected individuals—In order to model normal patterns of craniofacial integration, we used a sample of CT images of unaffected infants without history of a craniofacial anomaly (Table 1). Each individual underwent a head CT study due to unexplained seizures, suspected concussion, headaches, etc., and CT studies for all unaffected individuals were negative for craniofacial anomalies. The unaffected sample is divided into a 'younger' sample (n = 14) ranging in age from 12 to 31 weeks, and an 'older' sample (n = 8) ranging in age from 33 to 81 weeks. The data are cross-sectional; we have only a single scan for each individual.

Unilateral cleft lip and palate—The phenotypic clinical entity of UCLP has been well described and the osseous deformity of these patients has recently been quantified using three-dimensional (3D) CT. Kane et al. (19) found a significant degree of osseous asymmetry between the two sides of the face in UCLP, especially in those areas closest to the cleft. These results agree with previous studies of UCLP using cadavers, dental models, anthropometry and cephalometry.

Pre-operative high resolution 3D CT scans were acquired on infants with complete UCLP (n = 28; ♂ = 15, ♀ = 13), all of Taiwanese Chinese ethnicity prior to primary repair of the lip. Sexes were combined for analysis. The mean age at time of pre-op CT scan was 13 weeks (Table 1). Variation in the distribution of the cleft position (right = 9, left = 19) was controlled by analysing data from the affected side of each patient.

Unilateral cleft lip and palate children underwent lip taping and placement of an acrylic feeding plate from early infancy and nine of the patients underwent nasoalveolar moulding treatment. All UCLP patients underwent a modified Millard lip repair and nasal correction using previously described methods (21) by the same surgeon at 36 weeks at Chang Gung Memorial

Hospital in Taipei, Taiwan. Post-operative head CT scans were obtained after soft tissue repair of lip and nose but just prior to palatoplasty (mean age at postoperative scan = 47 weeks). Data from these scans has been previously reported (19,22,23).

Sagittal craniosynostosis—Premature fusion of the sagittal suture results in a dolichocephalic skull and accounts for 40–58% of all craniosynostosis cases. Our mixed cross-sectional sample consists of 17 pre-operative and nine postoperative cranial CT scans of children with ISS (Table 1) and includes a subset of infants for whom we have both pre- and post-operative data. Pre-operative CT scans were taken just prior to the initial surgery, and the post-operative CT scans were taken approximately 1 year (43–90 weeks) after surgery. All patients were males, except for two post-operative female patients. Ethnicity of these patients is unknown.

All patients for whom we have post-operative head CT scans had undergone craniectomies, cranial expansions or a combination of both. Our purpose is not to differentiate among operative procedures on the basis of outcome, but rather to determine the generalized effect that the removal of the constraint of the fused sagittal suture has on the integration of cranial base measures. Data from these samples have been previously analysed and reported (11,24).

Landmark coordinate data—Three-dimensional surface reconstructions were produced from the CT image slice data, and the 3D coordinate locations of landmarks located on the cranial vault, cranial base and facial skeleton (Table 2, Fig. 1) were recorded using eTDIPS, a multi-dimensional volume visualization and analysis software (http://www.cc.nih.gov/cip/software/etdips/). Anatomical landmarks are biologically meaningful, specific loci that can be repeatedly located with a high degree of accuracy and precision (25,26). Detailed anatomical definitions for the landmarks can be found on the landmark page of the Richtsmeier laboratory website, (http://www.getahead.psu.edu/landmarks_new.html). Measurement error for these 3D landmark data sets was evaluated following methods presented previously (27,28) and minimized statistically by digitizing each specimen two times, checking for overt error (e.g. mislabelling of left and right sides), and using the average of two data collection trials to reduce intra-observer error.

Sets of linear distances comprising dimensions of the cranial vault, cranial base and face were calculated from the landmark coordinates of each individual and a set of 22 linear distances (Table 3) were used in all but one analysis. Imaging protocols for a portion of the post-operative ISS sample excluded imaging of the lower face, resulting in 3D CT scans that included different portions of the face. In addition, neurocranial surgery artificially modifies the location of most vault landmarks. Consequently, the set of linear distances used in the comparative analysis of the pre- and postoperative ISS sample is limited to the set representing only the cranial base.

Research design

Our analysis is designed to answer the set of research questions given below (see Fig. 2).

Research question 1—In the unaffected sample, what is the pattern of MI within cranial base, vault and face, and between these anatomic regions?

We compare the younger, unaffected infants to the older unaffected individuals. Our null hypothesis is that MI remains constant over the time period considered here:

$$H_0 1A: MI_{cranium}(\text{young unaffected}) = MI_{cranium}(\text{older unaffected})$$

Research question 2—How does a craniofacial defect affect patterns of craniofacial MI?

We compare the young unaffected sample with: 1) the pre-operative UCLP sample; 2) the pre-operative sagittal synostosis sample. Our null hypothesis for these analyses is that the pattern of MI is similar across all groups within the younger age grouping:

$$H_0 2A\ \text{Facial defect:}MI_{cranium}(\text{young unaffected}) = MI_{cranium}(\text{pre} - \text{op UCLP})$$
$$H_0 2B\ \text{Neurocranial defect:}MI_{cranium}(\text{young unaffected}) = MI_{cranium}(\text{pre} - \text{op ISS})$$

Racial affinity is unknown for our unaffected and sagittal synostosis individuals, but all individuals in the UCLP samples are Taiwanese Chinese. Because the effect of racial affinity on patterns of MI is unknown we acknowledge that it may be a factor in these analyses.

Research question 3—How does surgery affect MI within the cranial base and what does this tell us about how the cranial base responds to surgery?

Within each dysmorphic sample we compare patterns of MI between pre- and post-operative cases focusing specifically on the cranial base. In the UCLP analysis data are available from the face, cranial vault and cranial base. In the ISS sample however, analysis is limited to the cranial base as the vault is directly manipulated during reconstructive surgery and the face is not consistently imaged in the post-operative sample. Our null hypothesis is that patterns of MI of the cranial base are unaffected by surgical intervention.

$$H_0 3A\ \text{Facial defect:}MI_{cranium}(\text{pre} - \text{op UCLP}) = MI_{cranium}(\text{post} - \text{op UCLP})$$
$$H_0 3B\ \text{Neurocranial defect:Ho:}MI_{base}(\text{ISS pre} - \text{op}) = MI_{base}(\text{ISS post} - \text{op})$$

Methods of analysis: MI

Morphological integration is estimated as the magnitude and pattern of correlation among measures. Although many analyses are used to study MI (17), we apply a method specifically designed to statistically compare MI patterns (correlation matrices) across groups (29). This method is based on the statistical analysis of the differences between the elements of two correlation matrices. Linear measures are first transformed to natural logarithms and then correlation matrices are estimated for each sample and compared by subtracting the elements of one matrix from the corresponding elements of the other matrix. If the relationship within and between various anatomical regions are the same, the correlation matrices are the same (the null hypothesis), and the differences for each element of the correlation difference matrix are expected to be zero. If the matrices are not similar, a statistical evaluation of differences in MI is performed by the estimation of nonparametric confidence intervals ($\alpha \leq 0.10$) for each linear distance pair. If the confidence interval excludes zero, we can reject the null hypothesis of similarity in MI. The statistical details of this bootstrap methodology developed by Cole (30) are described by Richtsmeier et al. (31).

Results

Normal patterns of MI

Younger vs. older unaffected—We first evaluated the average magnitude of integration among modules of the cranium (Table 4). In the younger unaffected samples, strength of MI

as measured by magnitude of the correlation is similar across all modules, though strongest in the cranial base. The magnitude of the average correlation is similar between younger and older unaffected individuals within the cranial base and vault, but decreases in magnitude in the face (Table 4).

We statistically compared correlation matrices between younger unaffected individuals and older unaffected individuals using our bootstrap approach. Of the 231 correlation coefficients for paired linear distances, 33 (14.3%) showed significant differences in correlation between the younger and older unaffected samples. The distribution of these significant differences among the three cranial modules is shown in Table 5. We were unable to reject the null hypothesis of equivalent integration for most of the linear distances in the cranial vault and base. In general, patterns of MI within these regions do not change with age. However, the pattern of integration within the face does changes during this period revealing seven significant differences in correlation values among measures within the face. Most of the facial distances that show significant difference between young and old unaffected samples include the endpoints zms and fzj, both of which are located on the orbit (Fig. 3). We suggest that the significant differences in integration patterns reveal changes in the relationship of the orbit to the rest of the face during growth. The globe of the eye follows a growth pattern more similar to that of the brain than to other facial organs. Significant differences between the younger and older unaffected samples represent relationships between orbits and cranial base or orbits and cranial vault (Table 5, Fig. 3).

MI of a facial anomaly: UCLP

Younger unaffected vs. pre-operative UCLP—The average magnitude of integration within all regions of the skull is reduced in the pre-operative UCLP sample relative to our ‘younger’ unaffected sample (Table 4). In the pre-operative UCLP sample, the magnitude of integration is strongest in the cranial base, followed by the vault and weakest in the face. Thirty-nine of the 231 linear distance pairs (16.9%) showed significant differences in correlation patterns between these two samples (Table 5). The pattern of integration within the cranial base was essentially unchanged (with the exception of one linear distance pair). In contrast, the pattern of integration within the cranial vault, within the face, and between the face and other portions of the cranium was significantly different for a large proportion of linear distance pairs. Many of these changes involve the landmark pterion posterior (ptnp), located in an area where the face, cranial base and calvaria meet. This suggests that changes in the face of pre-operative UCLP infants are being accommodated by adjustments in the regions that provide a structural connection between the face and cranial base.

MI of a calvarial anomaly: isolated sagittal synostosis

Younger unaffected vs. pre-operative ISS—There is a general reduction in the magnitudes of MI in the pre-operative ISS individuals, relative to those values computed for unaffected individuals (Table 4). This was particularly notable for integration within the face and for integration of face with cranial base, although integration within the cranial base remained high. Thirty of the 231 correlations (13.0%) are significantly different between the younger unaffected and ISS pre-operative samples (Table 5). Statistical testing of differences in patterns of integration between younger unaffected and pre-op ISS infants reveals a similarity in the pattern of integration within the cranial base. A few significant differences in MI within the vault and face are revealed, but most of the significant differences in correlations represent linear distance pairs that include one dimension from the cranial vault and one dimension from the face. This suggests an increased need for local alterations in facial and cranial vault dimensions when the sagittal suture is prematurely fused. Our results reveal that significant changes in association between cranial base and face also occur when the sagittal suture is closed prematurely.

The effect of surgery on the cranial base

Facial surgery: pre-op vs. post-up UCLP—Morphological integration within the three modules of the skull show remarkable stability between the pre-and post-operative UCLP samples (Table 5). The correlation of a single linear distance pair within the face is significantly different in the comparison of pre- and post-operative UCLP samples and no significant differences in MI patterns occur within the cranial vault and base. Although the average magnitude of correlation within face and cranial vault is decreased in pre-operative incidences of UCLP relative to the unaffected sample (see Younger unaffected vs. pre-operative ISS), the magnitude and pattern of MI after soft tissue repair of the lip and nose remain stable in all regions.

Cranial vault surgery: pre-op vs. post-op ISS—This comparison, limited to analysis of the cranial base, reveals a substantial reduction in the magnitudes of correlations in the post-operative sample. Of the 21 linear distance pairs in the cranial base, five (24%) showed significant differences between the pre- and post-op ISS samples. These results indicate that surgical intervention on the vault produces a significant disruption in MI of the cranial base. Close examination of our results (data not shown) reveal decreased integration in ISS postoperative crania between that part of the cranial base anterior to the foramen magnum and aspects of the most inferior portion of the posterior cranial fossa (Fig. 4).

Discussion

The concept of MI reflects the association within and among parts. These parts are often described as modules, consisting of a suite of characters that are more tightly integrated internally than they are with other character suites, and that operate largely independently of other characters (17,32–37). Integration and modularity are highly related concepts (36,38). If we look at the human skull, we can appreciate it as an integrated whole, a module in a sense that is integrated with the vertebral column and other modules of the post-cranial skeleton. However, the skull can be thought of as consisting of a series of integrated modules. In designing this study, we used a traditional view of craniofacial compartmentalization separating the skull into cranial base, cranial vault and facial skeleton. We found that integration of the cranial base was extremely stable and changed only when an abrupt structural insult (ISS surgery) occurred. As the surgery involved direct manipulation of the cranial vault but disrupted integration of the cranial base, we conclude that these two modules interact with one another especially when changes in the vault are abrupt. Our data suggest that when changes to the vault occur gradually over developmental time, as in ISS, adjustments are made to growth trajectories in the base that do not disrupt integration patterns. However, both the cranial vault and facial skeleton experience reduced integration in ISS.

Relative to unaffected individuals, MI of face and vault is profoundly altered in UCLP, most likely due to redirected growth related to the presence of a frank osseous cleft. Much has been written about the influence of the pressures of nasal soft tissue and lip repair on the disarticulated portions of the palate (23,39–43). Although subsequent soft tissue repair improves the outward appearance of the individual, it does not affect MI among the bones of the face, or the relationship of the face to other parts of the skull.

Sagittal synostosis impacts patterns of MI primarily in the face and vault, leaving patterns of integration within the cranial base conserved relative to unaffected individuals. However, significant differences in the pattern of integration within the cranial base become apparent after surgical correction of the cranial vault. Our previous studies of growth of the cranial base in ISS following vault surgery supported the supposition that ISS results in an over-rotation of the posterior cranial fossa and that this over-rotation resolves after vault surgery (11). Although craniosynostosis surgery is done to ‘normalize’ the appearance of the cranial vault, our analysis

indicates that the surgery does not normalize the relationships of measures within the cranial base, but instead disrupts a system. We stress the finding of stable integration of the cranial base in sagittal synostosis and its dissolution when the vault is surgically altered because it infers a transmission of information between the two modules. Communication between vault and base could be occurring across bones that connect these two osseous regions, but could also be transmitting information via the brain and the dura mater that provide a continuous union between vault and base. Previous research has shown that the dura is involved in maintenance of suture patency (44), and it is known that the shape of the cranial base and vault are determined by the growing brain. Our hypothesis is that release of the sagittal suture by surgical means results in an abrupt change in brain shape. That change is contained, and perhaps mediated by the dura mater, which is disconnected from the cranial vault at surgery, but remains tightly adhered to the cranial base at the lesser wings of the sphenoid, crista galli, along the crest of the petrous temporal (45,46) and perhaps at other anatomical locations. Whether changes resulting from vault surgery are transmitted biomechanically or by some other means of cell–cell or tissue–tissue interaction is unknown at this time, but our analysis shows that adjustments within the cranial base occur following vault surgery.

Conclusions

In general, we have found that ISS and UCLP disrupt normal patterns of MI of the face and vault, usually decreasing the magnitude of integration, while integration within the cranial base is relatively stable even when facial or vault dysmorphogenesis occurs. Stable integration of the cranial base may be required to insure the protection of neurovascular pathways and allow its function as a keystone supporting both face and vault. The processes that establish and administer these relationships are unknown.

Our analysis provides further support for the dynamic communication between various aspects of the skull during normal and abnormal development and following surgical manipulation. Although this study considered only the skeletal components of these modules, we propose that an understanding of the within- and between module adjustments will require study of all cranial tissues, soft and osseous.

Acknowledgments

This analysis could not have been done without the help of our surgical co-investigators: Dr Jun-Lou Lo (Chang Gung Memorial Hospital, Taiwan), Dr Alex Kane (Washington University Medical Center, St Louis, MO), Dr Jeffrey Marsh (St John's Mercy Medical Center, St Louis, MO), Dr Jayesh Panchal (University of Oklahoma Medical Center, Oklahoma City, OK), Dr Craig VanderKolk (Mercy Medical Center, Baltimore, MD) and Dr Ben Carson (Johns Hopkins Medical Center, Baltimore, MD). We thank David Covell for his invitation to present our work and for his efforts in organizing the COAST program and in putting together these volumes. Space restrictions limited our cited literature. We apologize to the authors of relevant literature that we could not cite. This work was supported in part by public service grants 1P60 DE 13078, R01 DE018500, R01 DE016886, R01 DD000350 and BCS-0234565 from the National Science Foundation.

References

1. Chai Y, Maxson RE Jr. Recent advances in craniofacial morphogenesis. Dev Dyn 2006;235:2353–75. [PubMed: 16680722]
2. Depew MJ, Simpson CA, Morasso M, Rubenstein JL. Reassessing the Dlx code: the genetic regulation of branchial arch skeletal pattern and development. J Anat 2005;207:501–61. [PubMed: 16313391]
3. Kuratani S. Craniofacial development and the evolution of the vertebrates: the old problems on a new background. Zoolog Sci 2005;22:1–19. [PubMed: 15684579]
4. Anton SC. Intentional cranial vault deformation and induced changes of the cranial base and face. Am J Phys Anthropol 1989;79:253–67. [PubMed: 2662783]

5. Cheverud JM, Kohn LA, Konigsberg LW, Leigh SR. Effects of fronto-occipital artificial cranial vault modification on the cranial base and face. Am J Phys Anthropol 1992;88:323–45. [PubMed: 1642320]
6. Konigsberg LW, Kohn LA, Cheverud JM. Cranial deformation and nonmetric trait variation. Am J Phys Anthropol 1993;90:35–48. [PubMed: 8470754]
7. Abramson DL, Janecka IP, Mulliken JB. Abnormalities of the cranial base in synostotic frontal plagiocephaly. J Craniofac Surg 1996;7:426–8. [PubMed: 10332261]
8. Burrows AM, Richtsmeier JT, Mooney MP, Smith TD, Losken HW, Siegel MI. Three-dimensional analysis of craniofacial form in a familial rabbit model of nonsyndromic coronal suture synostosis using Euclidean distance matrix analysis. Cleft Palate Craniofac J 1999;36:196–206. [PubMed: 10342607]
9. Mooney MP, Siegel MI, Burrows AM, Smith TD, Losken HW, Dechant J, et al. A rabbit model of human familial, nonsyndromic unicoronal suture synostosis. I. Synostotic onset, pathology, and sutural growth patterns. Childs Nerv Syst 1998;14:236–46. [PubMed: 9694335]
10. Smith TD, Mooney MP, Burrows AM, Losken HW, Siegel MI. Postnatal changes in the cranial base in rabbits with congenital coronal suture synostosis. J Craniofac Genet Dev Biol 1996;16:107–17. [PubMed: 8773901]
11. DeLeon VB, Zumpano MP, Richtsmeier JT. The effect of neurocranial surgery on basicranial morphology in isolated sagittal craniosynostosis. Cleft Palate Craniofac J 2001;38:134–46. [PubMed: 11294541]
12. Marsh JL, Vannier MW. Cranial base changes following surgical treatment of craniosynostosis. Cleft Palate J 1986;23(Suppl 1):9–18. [PubMed: 3469046]
13. Perlyn CA, Marsh JL, Pilgram TK, Kane A. Plasticity of the endocranial base in nonsyndromic craniosynostosis. Plast Reconstr Surg 2001;108:294–301. [PubMed: 11496166]
14. Olson, E.; Miller, R. Morphological Integration. Chicago, IL: The University of Chicago Press; 1958.
15. Olson, E.; Miller, R. Morphological Integration. Chicago, IL: University of Chicago Press; 1999.
16. Pigliucci, M.; Preston, K., editors. Phenotypic Integration: Studying the Ecology and Evolution of Complex Phenotypes. New York: Oxford University Press; 2004.
17. Klingenberg CP. Morphological integration and developmental modularity. Annu Rev Ecol Evol Syst 2008;39:115–32.
18. Magwene P. New tools for studying integration and modularity. Evolution 2001;55:1734–45. [PubMed: 11681729]
19. Kane AA, DeLeon VB, Valeri C, Becker DB, Richtsmeier JT, Lo LJ. Preoperative osseous dysmorphology in unilateral complete cleft lip and palate: a quantitative analysis of computed tomography data. Plast Reconstr Surg 2007;119:1295–301. [PubMed: 17496604]
20. Richtsmeier JT, Cole TM III, Krovitz G, Valeri CJ, Lele S. Preoperative morphology and development in sagittal synostosis. J Craniofac Genet Dev Biol 1998;18:64–78. [PubMed: 9672839]
21. Noordhoff M, Chen Y, Chen K, Hong K, Lo LJ. The surgical technique for the complete unilateral cleft lip-nasal deformity. Oper Techn Plast Reconstr Surg 1995;2:167–74.
22. DeLeon, V.; Kane, AA.; Valeri, CJ.; Richtsmeier, JT.; Lo, LJ. The effects of growth and lip repair upon osseous facial morphology in unilateral complete cleft lip and palate: an analysis of longitudinal CT data. In: Lilja, J., editor. Transactions of the 9th International Congress on Cleft Palate and Related Craniofacial Anomalies. Götenburg: Elanders Novum; 2001. p. 293-8.
23. Seidenstricker-Kink LM, Becker DB, Govier DP, Deleon VB, Lo LJ, Kane AA. Comparative osseous and soft tissue morphology following cleft lip repair. Cleft Palate Craniofac J 2008;45:511–7. [PubMed: 18788869]
24. DeLeon V, Richtsmeier JT. Fluctuating asymmetry and developmental instability in sagittal craniosynostosis. Cleft Palate Craniofac J 2009;46:187–96. [PubMed: 19254065]
25. Lele, S.; Richtsmeier, J. An invariant approach to the statistical analysis of shapes. Boca Raton, FL: Chapman & Hall/CRC; 2001. p. 308
26. Richtsmeier JT, Paik CH, Elfert PC, Cole TM III, Dahlman HR. Precision, repeatability, and validation of the localization of cranial landmarks using computed tomography scans. Cleft Palate Craniofac J 1995;32:217–27. [PubMed: 7605789]

27. Aldridge K, Boyadjiev SA, Capone GT, DeLeon VB, Richtsmeier JT. Precision and error of three-dimensional phenotypic measures acquired from 3dMD photogrammetric images. Am J Med Genet A 2005;138A:247–53. [PubMed: 16158436]
28. Valeri CJ, Cole TM III, Lele S, Richtsmeier JT. Capturing data from three-dimensional surfaces using fuzzy landmarks. Am J Phys Anthropol 1998;107:113–24. [PubMed: 9740305]
29. Cole T III, Lele S. Bootstrap-based methods for comparing morphological integration patterns. Amer J Phys Anthopol, Suppl 2002;34:55.
30. Cole, T, III. MIBoot Windows-Based Software for Bootstrap-Based Comparison of Morphological Integration Patterns. Richtsmeier Lab; 2002. Available at: http://getahead.psu.edu
31. Richtsmeier JT, Aldridge K, DeLeon VB, Panchal J, Kane AA, Marsh JL, et al. Phenotypic integration of neurocranium and brain. J Exp Zool B Mol Dev Evol 2006;306:360–78. [PubMed: 16526048]
32. Depew MJ, Compagnucci C. Tweaking the hinge and caps: testing a model of the organization of jaws. J Exp Zool B Mol Dev Evol 2008;310:315–35. [PubMed: 18027841]
33. Depew MJ, Simpson CA. 21st century neontology and the comparative development of the vertebrate skull. Dev Dyn 2006;235:1256–91. [PubMed: 16598716]
34. Gasser, G.; Bolker, J. Modularity. In: Olson, W.; Hall, B., editors. Keywords and Concepts in Evolutionary Developmental Biology. Cambridge: Harvard University Press; 2002. p. 260-7.
35. Jiang X, Liu B, Jiang J, Zhao H, Fan M, Zhang J, et al. Modularity in the genetic disease–phenotype network. FEBS Lett 2008;582:2549–54. [PubMed: 18582463]
36. Klingenberg C, Badyaev A, Sowry S, Beckwith N. Inferring developmental modularity from morphological integration: analysis of individual variation and asymmetry in bumblebee wings. Amer Nat 2001;157:11–23. [PubMed: 18707232]
37. Wagner G. Homologues, natural kinds and the evolution of modularity. Amer Zool 1996;36:36–43.
38. Willmore K, Young N, Richtsmeier JT. Phenotypic variability: its components, measurement, and underlying developmental mechanisms. Evol Biol 2007;34:99–120.
39. Aminpour S, Tollefson TT. Recent advances in presurgical molding in cleft lip and palate. Curr Opin Otolaryngol Head Neck Surg 2008;16:339–46. [PubMed: 18626253]
40. Li Y, Shi B, Song QG, Zuo H, Zheng Q. Effects of lip repair on maxillary growth and facial soft tissue development in patients with a complete unilateral cleft of lip, alveolus and palate. J Craniomaxillofac Surg 2006;34:355–61. [PubMed: 16859911]
41. Ogata H, Nakajima T, Onishi F, Tamada I, Hikosaka M. Cleft palate repair using a marginal musculomucosal flap. Cleft Palate Craniofac J 2006;43:651–5. [PubMed: 17105319]
42. Tollefson TT, Gere RR. Presurgical cleft lip management: nasal alveolar molding. Facial Plast Surg 2007;23:113–22. [PubMed: 17516338]
43. Wattanawong K, Tan YC, Lo LJ, Chen PK, Chen YR. Comparison of outcomes of velopharyngeal surgery between the inferiorly and superiorly based pharyngeal flaps. Chang Gung Med J 2007;30:430–6. [PubMed: 18062174]
44. Opperman LA. Cranial sutures as intramembranous bone growth sites. Dev Dyn 2000;219:472–85. [PubMed: 11084647]
45. Moss, M. The functional matrix. In: Kraus, B.; Reidel, R., editors. Vistas in Orthodontics. Philadelphia, PA: Lea and Febiger; 1962. p. 85-98.
46. Moss M, Young R. A functional approach to craniology. Amer J Phys Anthropol 1960;18:281–92. [PubMed: 13773136]

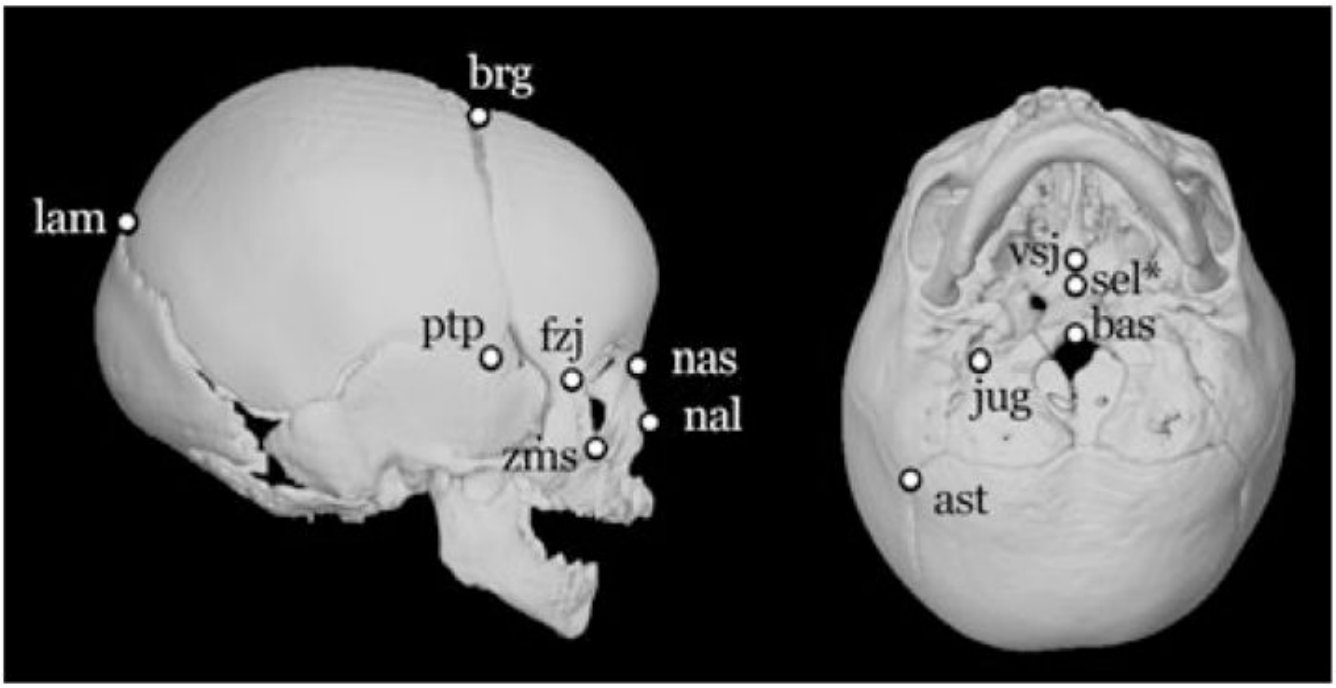

Fig. 1.
Twelve right-sided and midline landmarks located on 3D CT reconstructions (lateral view at left; ectocranial base at right) used in analysis. Landmark names are given in Table 2. *Sella (sel) is located endocranially, but its approximate location is shown on the ectocranial view.

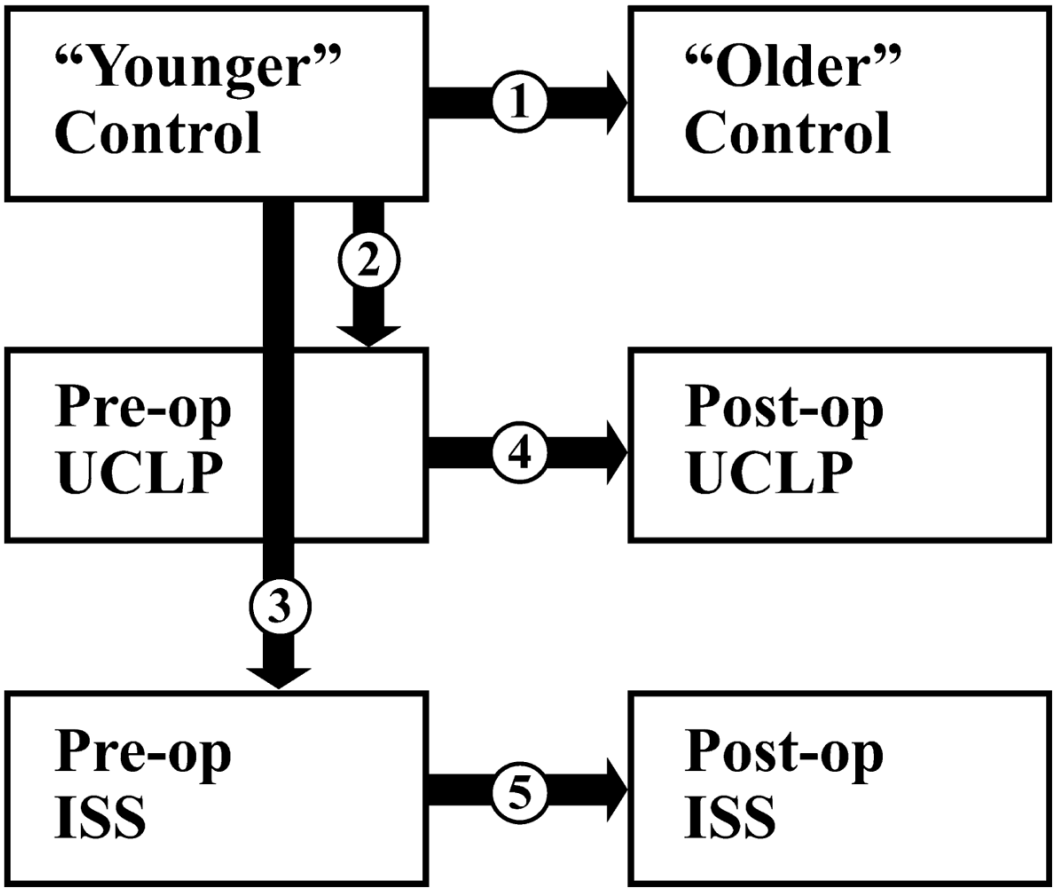

Fig. 2.
Graphic representation of our research design demonstrating the five comparisons between samples (boxes) used to test null hypotheses. See text for research questions and statement of null hypotheses.

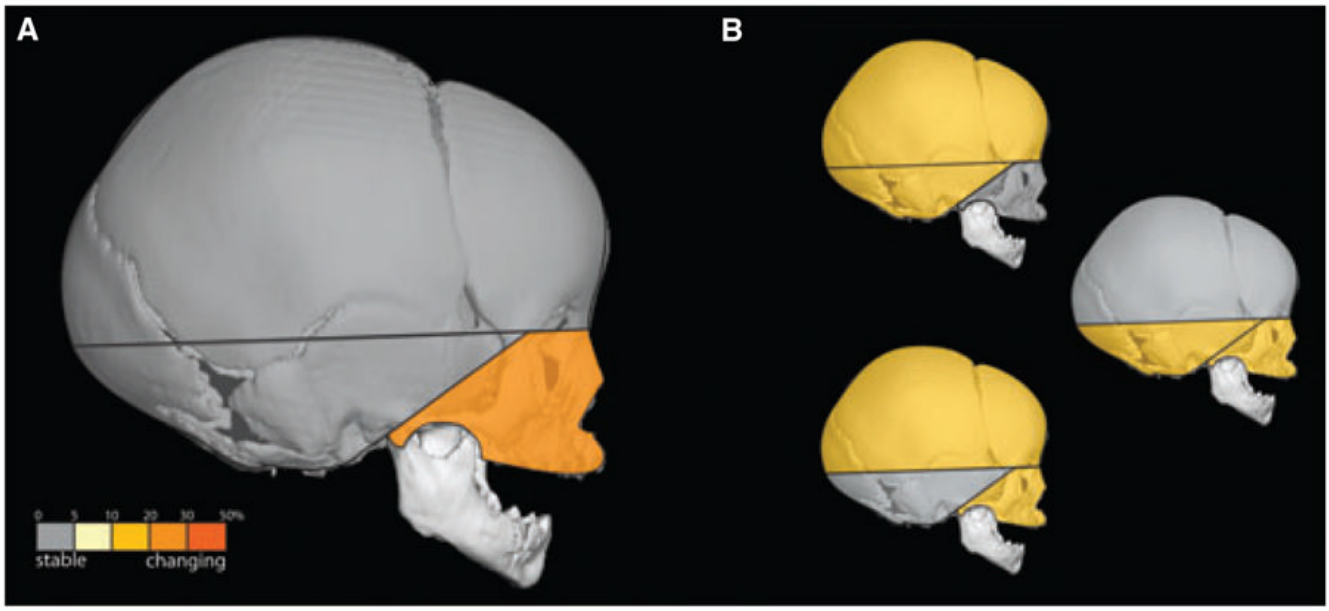

Fig. 3.
(A) Correlations within the face show the greatest number of significant differences in morphological integration between younger and older unaffected samples. There is no significant change within the cranial vault or within the cranial base. (B) Integration between measures from different modules shows a moderate number of significant differences.

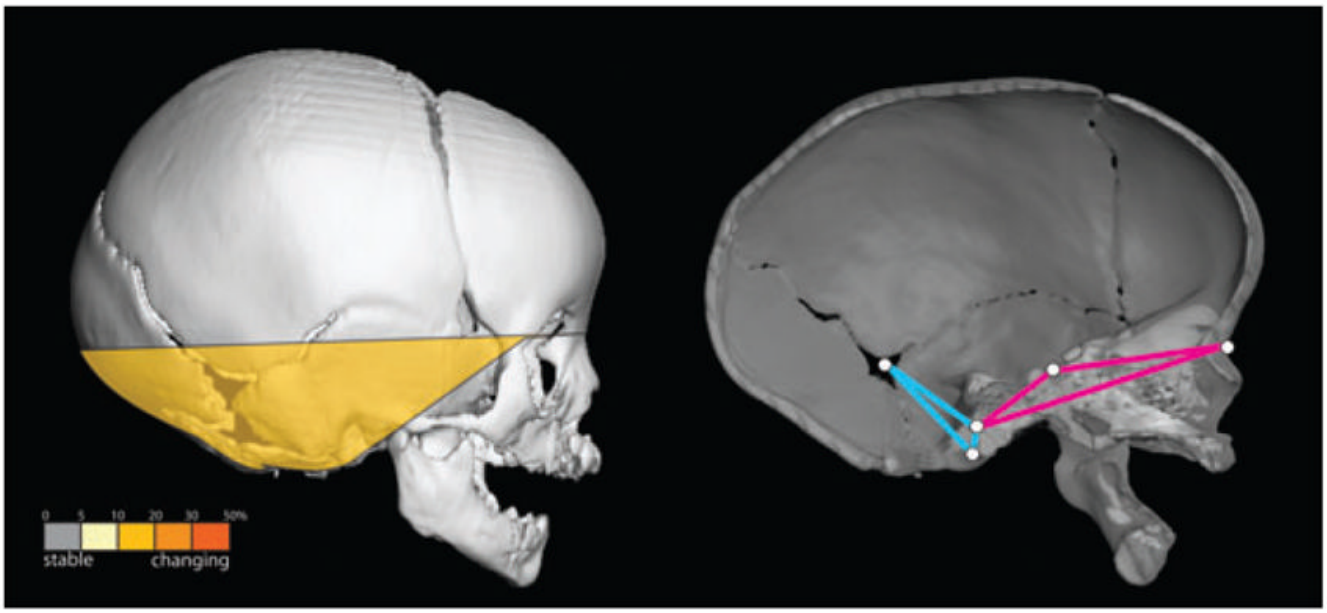

Fig. 4.

Linear distance pairs within the cranial base show significantly reduced integration in the post-operative ISS sample (left). Relative to the pre-operative ISS sample, the postoperative sample shows a marked reduction in the magnitude of morphological integration for linear distance pairs that include a measure from that portion of the cranial base anterior to foramen magnum (shown in pink) and a measure from the inferior portion of the posterior cranial fossa (shown in blue).

Table 1

Information pertaining to the image data used in these analyses

Study sample	Age range (weeks)	Sample size	Data type	References for further studies of data set
Young unaffected	12–31	14	Cross-sectional	24
Old unaffected	33–81	8		
Young UCLP pre-op	3–18	28	Longitudinal	19,22,23
Old UCLP post-op	40–58	28		22,23
Young SS pre-op	11–37	17	Mixed cross-sectional	11,24
Old SS post-op	66–96	9		11

Table 2

Landmarks used in this study

AST	Asterion
BAS	Basion
BRG	Bregma
FZJ	Frontomalare orbitale
JUG	Jugular process (anterior point)
LAM	Lambda
NAL	Nasale
NAS	Nasion
PTP	Pterion posterior (fronto-spheno-parietal intersection)
SEL	Centre of sella turcica (on bone)
VSJ	Hormion (posterior midline point on vomer)
ZMS	Zygomaxillare superior

See Fig. 1 for landmark location on the skull.

Table 3

Modules and their linear distances (right side only)

Face	Cranial vault	Cranial base
zms-nas	nas-brg	nas-sel
nas-nsl	nas-ptp	nas-bas
nsl-zms	brg-ptp	sel-jug
fzj-nas	brg-ast	sel-bas
fzj-zms	brg-lam	jug-bas
vsj-nas	ptp-ast	bas-ast
vsj-zms	ast-lam	jug-ast
vsj-fzj		

Table 4

Average correlation values within and between cranial modules: CB, CV and FACE

	CB	CV	FACE
Young unaffected			
CB	0.63		
CV	0.49	0.58	
FACE	0.58	0.49	0.60
Old unaffected			
CB	0.60		
CV	0.52	0.58	
FACE	0.48	0.42	0.34
Pre-op UCLP			
CB	0.53		
CV	0.43	0.40	
FACE	0.44	0.34	0.33
Post-op UCLP			
CB	0.52		
CV	0.39	0.30	
FACE	0.40	0.28	0.35
Pre-op ISS			
CB	0.60		
CV	0.53	0.51	
FACE	0.39	0.41	0.44
Post op ISS (CB only)			
CB	0.19		
CV	NA	NA	
FACE	NA	NA	NA

CB, cranial base; CV, cranial vault; FACE, facial skeleton; UCLP, unilateral cleft lip and palate; ISS, isolated sagittal craniosynostosis.

The number in each cell represents the absolute value of the average correlation coefficient among linear distance pairs within each of the modules and between modules. Analysis of the post-op ISS sample is limited to CB.

Table 5

Statistical comparison of morphological integration patterns

	CB	CV	FACE
Younger unaffected → older unaffected			
CB	0		
CV	6 (12.2)	1 (4.8)	
FACE	9 (16.1)	10 (17.9)	7 (25.0)
Younger unaffected → pre-op UCLP			
CB	1 (4.8)		
CV	6 (12.2)	7 (33.3)	
FACE	5 (8.9)	10 (17.9)	10 (35.7)
Pre-op UCLP → post-op UCLP			
CB	0		
CV	2 (4.1)	0	
FACE	3 (5.4)	1 (1.8)	1 (3.6)
Younger unaffected → pre-op ISS			
CB	0		
CV	2 (4.1)	4 (19.0)	
FACE	6 (10.7)	14 (25.0)	4 (14.3)
Pre-op ISS → post-op ISS			
CB	5 (23.8)		
CV	NA	NA	
FACE	NA	NA	NA

CB, cranial base; CV, cranial vault; FACE, facial skeleton; UCLP, unilateral cleft lip and palate; ISS, isolated sagittal craniosynostosis.

For each comparison, cells of the matrix contain the number of linear distance pairs with significantly different levels of morphological integration (given as a percentage in parentheses).